CARITAS UNIVERSITY AMORJI-NIKE, EMENE, ENUGU STATE
Caritas Journal of Engineering Technology
CJET, Volume 4, Issue 1 (2025)
Article History: Received:12th April, 2025 Revised: 2nd June, 2025 Accepted:10th June, 2025

A Comprehensive Pressure Distribution Model for Horizontal Well in Bottom-Water Reservoir

Ogbue, M.C.
Department of Petroleum Engineering,
Delta State University, Abraka, Oleh Campus, P.M.B. 22, Oleh, Delta State, Nigeria.
Corresponding author: mogbue@delsu.edu.ng

Abstract
The growing application of horizontal well technology provided far-reaching solutions to more realistic phenomena in well test analyses. However, existing models restrict the types of flow regimes by assuming that the dynamics of fluid are controlled by the geometry of the reservoir only. Such an assumption limits the number of flow regimes and hence the accuracy of well test analyses. In this article, all potential flow regimes of a horizontal well in a reservoir supported by bottom water were considered. The conceptual model assumed that the dynamics of the reservoir fluid are a function of the petrophysical properties of the reservoir, the properties of the fluid, and the geometry of the reservoir system. The physical model and the mathematical model were developed based on the conceptual model. The mathematical model is the pressure distribution of the horizontal well in the reservoir. The pressure distribution is in the form of dimensionless pressure and dimensionless pressure derivative functions of reservoir system properties, fluid properties, reservoir system geometry, and dimensionless time. Results of the study show a series of flow patterns along the principal axes or along combinations of the principal axes. Each flow regime could be distinguished by one of the flow patterns and the axes of orientation of the pattern. Each flow regime could be recognized by its characteristic signature in the log-log graph plots of the pressure distribution.

Keywords: ***Horizontal well, pressure distribution, model, unlimited flow regimes, bottom water boundary***

1.0 Introduction

Knowledge of fluid dynamics is fundamental to well test analyses procedures. Well test analysis is based on an interpretation of the pressure distribution of a well in a reservoir under a specified flow regime. Various studies have been undertaken to determine the transient flow behaviour of horizontal wells. Transient pressure analysis of a horizontal well with multiple, arbitrarily shaped horizontal fractures has been studied [1]. Pressure transient behaviour has been extended to layered reservoirs [2], [3], [4], [5], [6], and [7]. Horizontal well test design and interpretation methods have been established [8], [9]. However, existing models restrict the number of flow regimes by assuming that geometry alone determines the number of possible flow regimes. On such a basis, models have a maximum of six flow regimes in a full flow period [10], [11], [12], [13], [14], [15], [16], [17], [18]. A study of reservoirs as a function of both fluid and rock properties suggests more possible flow regimes.

Therefore, in this article, pressure distribution models containing other possible flow regimes, which hitherto have not been considered, were studied.

2. 0 Methodology

2.1 Conceptual Model

A horizontal well in a reservoir underlain by an active aquifer was chosen. The dynamics of reservoir fluid were selected to be a function of reservoir properties, fluid properties, and the geometry of the reservoir system. Three primary permeability axes, regarded as the x-axis, y-axis, and z-axis, were selected. The permeability along the primary axes was for the x-axis, y-axis, and z-axis, respectively.

2.2 Physical Model

The physical model that is cuboid in shape was selected and is shown in Figure 1 as a 2D reservoir system.

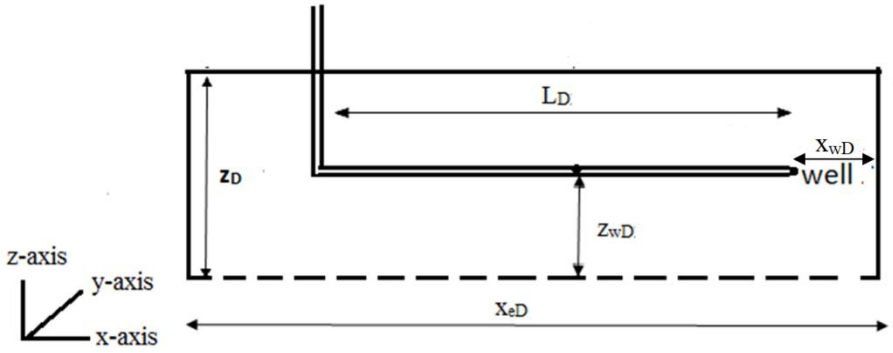

Figure 1: 2D Physical Model for Horizontal Well in a Reservoir Subject to Bottom Water Drive.

2.3 Mathematical Model

The mathematical model is the pressure distribution. It is in form of dimensionless pressure, P_D, and dimensionless pressure derivative, $P_D^{'}$. They are functions of reservoir system properties, fluid properties, reservoir system geometry and dimensionless time. A mathematical model was derived employing instantaneous source and Green's function proposed for constant-rate [22].

2.3.1. Description along Axis

Axial description of reservoir system was given so as to appropriately choose the functions.

a. Description of x- axis:

(i) The reservoir is bounded at both ends. (ii) The well length coincides with the x-axis. (iii) The well is an infinite slab source in an infinite slab reservoir. (v). Source number is x.

Description of y-axis:

(i) the reservoir is bounded at both ends. (ii). the well length does not coincide with the y-axis (iii) the well is an infinite plane source in an infinite slab reservoir. (iv) Source number.

b. Description of z-axis

(i) the reservoir is bounded at the top, and has pervious bottom. (ii). well length does not coincide with the z-axis. (iii). the well is an infinite plane source in an infinite slab reservoir. (iv). Source number ix (z)' which is a modified form of ix (z).

2.3.2. Mathematical Model in form of Dimensionless Expression

By using Newman product rule:

$$P_D = 2\pi h_D \int_0^{t_D} x(x).vii(y).ix(z)'d\tau \qquad (1)$$

So, Equation (1) can be written as Equation (2) showing for all possible flow regimes listed.

$$\begin{aligned} P_D = {} & 2\pi h_D \int_0^{t_{D1}} ii(x).i(y).i(z)d\tau \\ & + 2\pi h_D \int_{t_{D2}}^{t_{D3}} ii(x).i(y).i(z)d\tau \\ & + 2\pi h_D \int_{t_{D4}}^{t_{D5}} ii(x).i(y).ix(z)'d\tau + 2\pi h_D \int_{t_{D6}}^{t_{D7}} ii(x).vii(y).i(z) + 2\pi h_D \int_{t_{D8}}^{t_{D9}} ii(x).i(y).ix(z)'d\tau \\ & + 2\pi h_D \int_{t_{D10}}^{t_{D11}} ii(x).vii(y).i(z)d\tau + 2\pi h_D \int_{t_{D12}}^{t_{D13}} x(x).i(y).i(z)d\tau + 2\pi h_D \int_{t_{D14}}^{t_{D15}} ii(x).vii(y).ix(z)'d\tau \\ & + 2\pi h_D \int_{t_{D16}}^{t_{D17}} x(x).i(y).ix(z)'d\tau + 2\pi h_D \int_{t_{D18}}^{t_{D19}} x(x).vii(y).i(z)d\tau \\ & + 2\pi h_D \int_{t_{D20}}^{t_{Del}} x(x).vii(y).ix(z)'d\tau \qquad (2 \end{aligned}$$

Equation (2) is the late-time dimensionless expression. Before late time, a series of possible flow regimes occurred. Dimensionless pressure at any time of interest is a time superimposition of individual flow regimes that have existed up to the time of interest. Each flow regime is represented by an integrand, and the limits of the integration are the interval of its existence.

The dimensionless pressure derivative is shown in Equations (3) and (4)

$$P_D' = \frac{\partial P_D}{\partial log t_D} \qquad (3)$$

Equation (3) can be further written as Equation (4), showing all the flow regimes

$$P_D' = 2\pi h_D\{[ii(x).i(y).i(z)] + [ii(x).i(y).i(z)] + [ii(x).i(y).ix(z)'] + [ii(x).vii(y).i(z)] + [ii(x).i(y).ix(z)'] + [ii(x).vii(y).i(z)] + [x(x).i(y).i(z)] + [ii(x).vii(y).ix(z)'] +$$

$$[x(x).i(y).ix(z)'] + [x(x).vii(y).i(z)] + [x(x).vii(y).ix(z)']\} \quad (4)$$

3.0 Results and Discussion

Prior to results compilation, the model was verified based on existing literature.

3.1 Model Verification

Due to the complexity of the model of this article, a single model from literature would not sufficiently allow for comparison. Therefore, the validation was done in bits by comparing some parts of this model of this work with models in other literature that have similar instances. Verification was done with the Ozkan *et al.* [23] model. Data used are as shown in Table 3.

Table 3: Reservoir System Parameters used for Validation of Model using Ozkan *et al*. [23] model

Parameter	K_x, md	K_y, md	K_z, md	Q, bbl/day	μ, cp	r_w(ft)	h_x, ft
Value	122	315	12	5000	1.2	0.35	13500
Parameter	B_o, bbl/STB	h_y, ft	L. ft	Ø, %	C_t, psi^{-1}	h_z, ft	
Value	1.12	52	2626	24	$5.0x10^{-5}$	84	

A critical look at permeability values shown in Table 3 revealed that Ky > Kx > Kz. In addition, hx > hz > hy. Such a condition will make the boundary along the y-axis be felt earlier than others. In the same vein, a boundary along the z-axis will be felt earlier than a boundary along the x-axis. Also, the well length is short compared to the length of the reservoir. Flow will certainly be beyond the tips of the well in a short time.

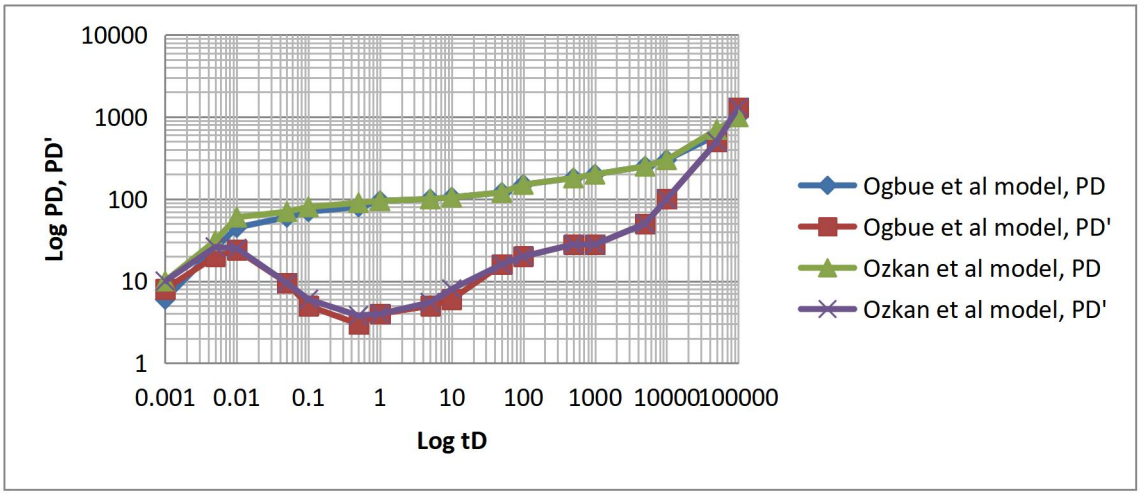

Figure 2: Plot of P_D, P_D' versus t_D for validation of Ogbue *et al.* model using Ozkan *et al*. [23] model.

Ogbu et al. model: Present study

As shown in Figure 2, early time radial flow, ERyz, was developing but short-lived, tD = 0.005 to 0.01. It stopped when the flow was beyond the tips of the well. Between tD = 0.01 and 1, ellipsoidal flow, EExyx, developed. Its characteristic signatures on the log-log plot of PD' were shown in Figure 2. However, due to the closeness of the boundary as well as high permeability along the axis, the y-axis was felt at about tD = 1. Since the y-axis is a closed boundary, PD and PD' simultaneously rose with time. That is the characteristic signature of linear flow, LLx. The curve obtained from the Ogbue et al. model compares well with the Ozkan et al. model, though higher values of PD, PD' were obtained at some point. There were points along the curve where the Ozkan model resulted in lower values. Data and models contained in the article by Goode *et al*. [9] were used for further verification, as shown in Table 4.

Table 4: Reservoir System Parameters used for Validation by Goode's model

Parameter	K_x, md	K_y, md	K_z, md	Q, bbl/day	μ, cp	r_w(ft)	h_x, ft
Value	50	100	25	3000	1.5	0.354	13500
Parameter	B_o, bbl/STB	h_y, ft	L. ft	Ø, %	C_t, psi^{-1}	h_z, ft	
Value	1.5	30	1000	10	$3.0x10^{-5}$	60	

Pressure distribution was modelled for a horizontal well in an anisotropic reservoir. The analytical solution results in this paper are compared with those in the report of Goode [9]. Basic data from Goode's paper are listed in Table 4. Permeability values were shown such that Ky > Kx > Kz, but the values are very close to each other. Also, hx > hz > hy, but the values of reservoir dimensions are very close for the y-axis and z-axis. Such a condition will make the boundary along the y-axis to be felt earlier than the other, but the boundary along the z-axis would be felt almost immediately. The boundary along the x-axis will be felt much later. Also, the well length is short compared to the length of the reservoir. Therefore, flow well certainly will be beyond the tips of the well in a short time. As shown in Figure 3, Goode's [9] solution was relatively small compared with the solution from this article.

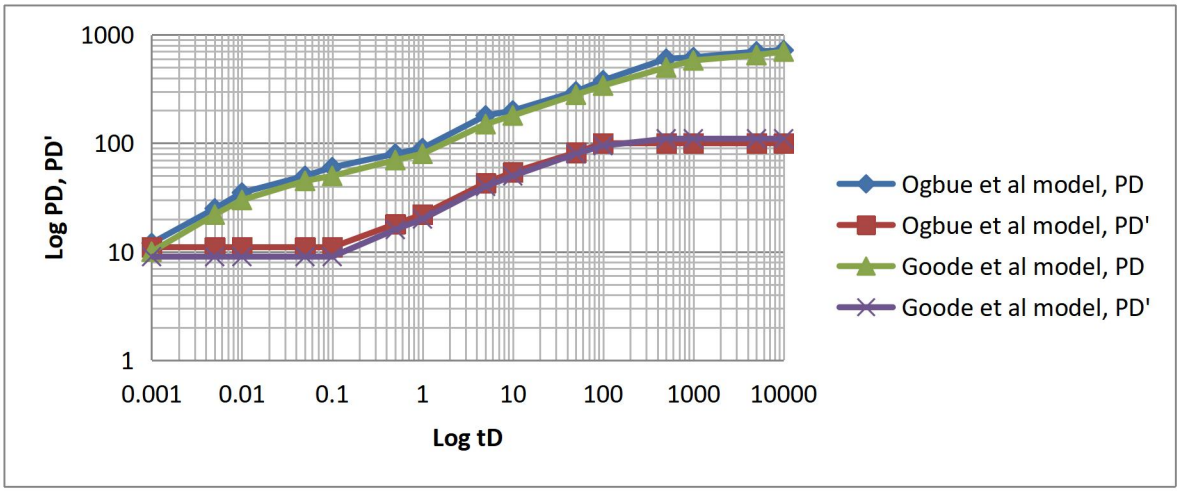

Figure 3: Comparison with the results from Ogbue's model and Goode's model on log-log plot.

Ogbue et al. model: Present study

With the values of input data, various flow regimes manifested. Each flow regime recognized by it characteristic signature. The various flow regimes obtained from Goode's model were observed to simulate some particular flow regimes, as indicated, that make up the model of this articles. Since wellbore was not considered in model of this article, that section for wellbore dominated period was overlooked. Characteristic signatures of early radial, ER_{yz}, was shown between $t_D = 0.001$ and 0.01. At about $t_D = 0.01$, characteristic signatures of early linear flow manifested and it lasted for the interval of $t_D = 0.01$ and 100. Since, y-axis could be more easily felt, flow was then linear along z-axis only, EL_z. Another radial flow was shown to manifest. Characteristic signatures of pseudo radial flow was observed at $t_D = 100$ lasted for the interval of $t_D = 100$ and beyond. Pseudo radial flow developed because flow along x-axis has gone beyond the tips of the well and flow was then along z-axis and x-axis leading to a pseudo radial flow, PR_{xz}. Similar characteristic signatures obtained have been documented in literature [3]. Further verification done with Viana *et al* [3] model and Mutisya *et al.* [25] model. Data used are as shown in Tables 5, 6, and 7.

Table 5: Reservoir System Parameters used for Validation of Model using Viana *et al* [3] model.

Case	r(m)	K(md)	h(m)	μ (cp)
A	16	1000	15	5.1
B	500	10	10	3.5

As shown in Figure 4, curves obtained from Case B march well with flow regime ERyz, tD = 0.0001 to 0.00. Another radial flow, pseudo-radial, PRxy, between tD = 0.001 and 10. Then boundary-dominated, BD, flow started at about tD = 10, and the boundary at the z-axis was observed. It was observed that the PD curve straightened horizontally, indicating a constant value; PD PD' slopes downwards, tending towards zero. While curves obtained from Case A match well with flow regime ERyz, tD = 0.0001 to 0.00. Another radial flow, pseudo-radial, PRxy, between tD = 0.001 and 10. Then boundary-dominated, BD, flow started at about tD = 10, and the boundary at the x-axis was felt. It was observed that the PD curve rose increasingly; PD's slopes rapidly upwards as well, indicating a no-flow boundary. PD values obtained from the model of this article were observed to be higher than those obtained from Viana et al. However, a close match was observed between the two models. Due to the presence of bottom water after tD = 1, PD for Case B was shown to increase slightly with time, while PD' started to slope downwards. However, for Case A, where the boundary is sealed, after tD = 1, PD was shown to increase rapidly with time, and PD' continued to increase rapidly with time too.

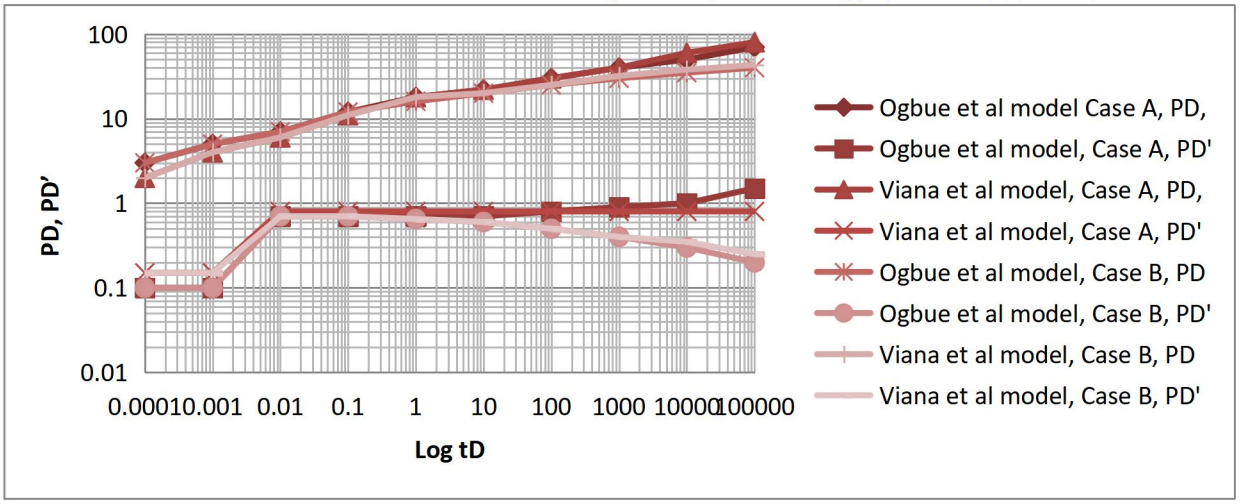

Figure 4: Comparison of results from Ogbue's model and Viana's [3] model for crossflow and no crossflow

Ogbue et al. model: Present study

A comparison was further carried out between the model of this study and the model of Mutisya *et al*. [25]. The parameters used are shown in Table 6.

Table 6: Reservoir System Parameters used for Validation of Model using Mutisya et al model, dimensioned parameters.

Case	L. ft	x_w, ft	y_w, ft	z_w, ft	Z, ft	x_e, ft	y_e, ft	z_e, ft	h, ft
A	500	134	200	160	160.5	6000	400	200	200
B	3500	134	200	160	160.5	6000	400	200	200
	dx, ft	dy, ft	dy, ft	Dx, ft	Dy, ft	Dz, ft	K_x, md	K_y, md	K_z, md
A	134	200	160	634	201	161	22	16	20
B	134	200	160	634	201	161	22	16	20

Permeability values were shown such that Ky > Kz > Ky, but the values are very similar to each other. Also, xe > ye > ze. Although values of reservoir dimensions are very close for the y-axis and z-axis, values of reservoir dimensions along the x-axis are several folds higher than the others. In a situation observed for the x-axis, where the permeability is not much higher than others but the distance of the boundary is much farther from the well than the distances of other boundaries. It is obvious that it will take a longer time before the boundary along the x-axis is felt. Such a condition will make the boundary along the z-axis be felt earlier than other boundaries. It is clear that the boundary along the y-axis would be felt almost immediately after the z-axis and the boundary along the x-axis much later. But the boundary-dominated effect of the z-axis will mask their effect. Boundary-dominated effect of the z-axis is a constant pressure boundary supported by bottom water. Well length is short compared to the length of the reservoir. So, flow well certainly will be beyond the tips of the well in a short time. The dimensionless parameters are shown in Table 7.

Table 7: Reservoir system parameters used for validation of model using Mutisya et al model, dimensionless parameters.

Case	L_D	x_{wD}	y_{wD}	z_{wD}	x_{eD}	y_{eD}	z_{eD}	h_D,
A	1.1669	0.5	0.8757	0.6266	22.404	1.7514	0.7832	0.7832
B	8.1681	0.5	0.1251	0.0056	3.1206	0.2502	0.028	0.1119
	x_D	y_D	z_D					
A	0.5	0.8757	0.6285					
B	0.5	0.1251	0.0059					

As shown in Figure 6, early time radial flow, ERyz, was developing but short-lived, tD = 0.01 to 0.1. It stopped when the flow got to the boundary along the z-axis. Boundary-dominated flow regime, BD, developed very early, tD = 0.1, due to the circumstances around the z-axis explained earlier. Its characteristic signatures on the log-log plot of PD were shown in Figure 8. It was observed that the PD curve straightened horizontally, indicating a constant value; PD'slopes downwards tending towards zero. This trend is consistent with the trend observed in literature [26].

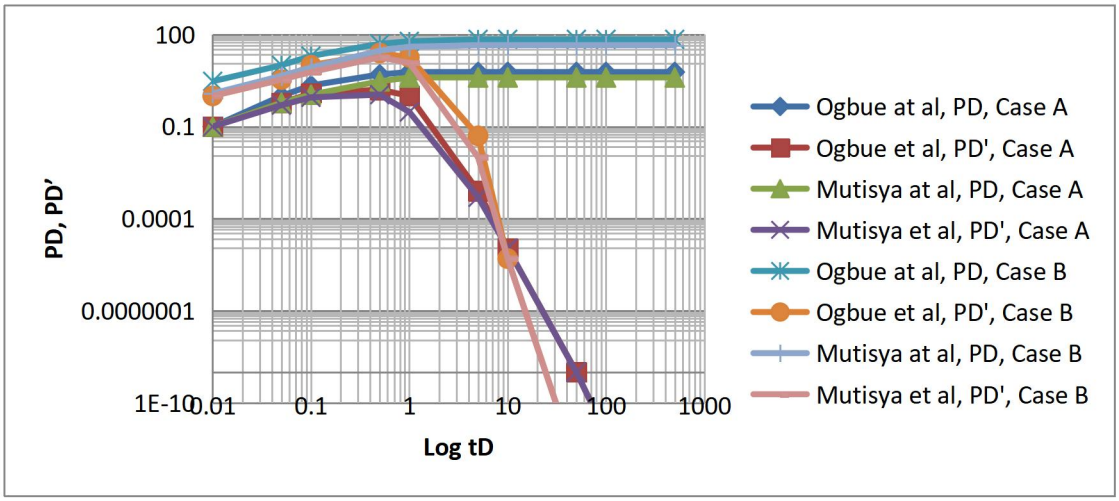

Figure 6: Comparison of results from the Ogbue *et al*. model and the Mutisya *et al.* [25] model on a log-log plot. *Ogbue et al. model: Present study*

In spite of the higher permeability along the y-axis, permeability could not compensate for the farther distance of the boundary to the well; hence, along the y-axis, it was not felt earlier than the z-axis. The curve obtained from the present study model compares well with the Mutisya *et al*. [25] model, though higher values of PD, PD' were obtained at some point. There were points along the curve where the Mutisya *et al*. [25] model had lower values.

.

3.2. Description of the Flow regimes

Some flow regimes cannot also co-exist. When two consecutive flow regimes overlap, only the one that was fully established was shown, while the other was masked.

ERyz: The flow is along the y- and z-axes but confined within the well along the x-axis flow. Early radial flow regime around the well length, provided flow has not gone beyond the tip of the well. During this time, flow along the x-axis is not affected by time, as flow is still within the well. It stops when flow is beyond the well or when any of the other external boundaries other than the x-axis are felt. Dimensionless pressure rises moderately with respect to dimensionless time. The slope of the log-log plot for the pressure derivative is constant; likewise, the dimensionless pressure derivative is constant.

EExyx: Flow along x, y, and z axes. It starts if there is sufficient time for flow to go beyond the tips of the well before any boundary is felt. This type of flow is an ellipsoidal flow regime. It occurs if well length is short compared to layer thickness along the other two axes or permeability values are comparatively closer to values along permeability along the axis of the well. The dimensionless pressure rises very sluggishly with time, while the dimensionless pressure derivative rises very moderately with time. It can be a symptomatic tool that suggests the need to extend producing well length. Deviated well completion is also a good alternative.

ELy: Flow along the y-y-axis. It occurs when only the top boundary has been felt. It occurs if the reservoir thickness is low compared with other dimensions of the reservoir or vertical permeability is relatively high. The dimensionless pressure tends to straighten horizontally, while the dimensionless pressure derivative declines rapidly and tends towards zero, thus indicating external energy. It obliterates spherical flow if it occurred.

ELz: Flow along the z-axis. It occurs when the boundary along the y-axis is felt first before other boundaries. It is possible when reservoir extent is closer along the y-axis or the permeability along that axis is relatively high. It obliterates spherical flow if it occurred.

PRxy: Flow along x- and y-axes. The flow pattern is radial at the top and bottom of the well. The dimensionless pressure rises at a constant rate, while the dimensionless pressure derivative straightens horizontally to a constant value.

PRxz: Flow along the x- and z-axes. This is the pseudo-radial flow regime. The flow pattern is radial at the tips or at the sides of the well. It is not as the real radial flow observed since the boundary effect has commenced. The dimensionless pressure rises at a constant rate, while the dimensionless pressure derivative straightens horizontally to a constant value.

PRyz: Flow along the y- and z-axes. This is given a pseudo-radial flow regime. The flow pattern is radial at the top or at the sides of the well. The dimensionless pressure rises at a constant rate, while the dimensionless pressure derivative straightens horizontally to a constant value.

LLx: Flow along the x-axis. The flow is late-time linear flow. The dimensionless pressure tends to rise rapidly, while the dimensionless pressure derivative also rises rapidly.

LLy: Flow along the y-y-axis. The flow is late-time linear flow. The dimensionless pressure and its rise rapidly indicate a completely sealed boundary.

LLz: Flow along the z-axis. At least boundaries along two axes have been felt. Another linear flow, late-time linear flow, is observed. The dimensionless pressure tends to a constant value, and its derivative declines towards zero, indicating a completely constant pressure boundary.

BD: All boundaries are felt, or the bottom boundary along the z-axis is felt. This is a complete boundary-dominated flow regime. The dimensionless pressure tends to a constant value, and its derivative declines towards zero, indicating a completely constant pressure boundary.

Conclusion

The inclusive pressure distribution of a horizontal well in a reservoir subject to bottom water has been presented in the form of a mathematical model. During a flow period, it is not possible for all the flow regimes to be experienced. The type of flow regime that would exist and its interval of existence are determined by the reservoir system parameters, architecture of the reservoir system, and the fluid properties. Unlike in most models in which the author decides the flow regime that occurs, the flow regime that may occur from the array of all the possible flow regimes and the duration of existence is determined by the values of parameters, geometry of the reservoir, fluid properties, and well architecture selected. The model was observed to produce a series of radial and linear flows along individual principal axes or combinations of any of the three principal axes. Each flow regime could be recognized by its characteristic signature in the log-log graph plots of the pressure, pressure derivative versus time, geometry of the reservoir system, and the petrophysical properties of the reservoir. The interval of existence depends on the reservoir system parameters. The existence of some flow regimes obliterates other flow regimes. Also, when the interval of subsistence is short, the flow regime is masked and not observed.

Acronyms:

ER Early radial

EE Early Ellipsoidal

EL Early linear

PR Pseudo radial

LL Late linear

BD Boundary dominated

Subscript

D dimensionless

e extremity of reservoir

w well

el economic limit

Nomenclature

h formation thickness, ft

L total length of horizontal well, ft.

x_e dimension of reservoir along x-axis

y_e dimension of reservoir along y-axis

z_e dimension of reservoir along z-axis

z_w distance between the external wall of well and the bottom/top of the reservoir

d_x shortest distance between the tip of the well and boundary of the x −axis, ft

d_y shortest distance between the well and boundary of the y −axis, ft

d_z shortest distance between the external wall of well and boundary of the z −axis, ft

D_x longest distance between the tip of the well and boundary of the x −axis, ft

D_y longest distance between the well and boundary of the y −axis, ft

D_z longest distance between the external wall of well and boundary of the z −axis, ft

Dimensionless Parameters

$$k = \sqrt[3]{k_x k_y k_z} \quad \text{..... 5}$$

$$h_D = \frac{2h}{L}\sqrt{\frac{k}{k_z}} \quad \text{..... 6}$$

$$L_D = \frac{L}{2h}\sqrt{\frac{k_x}{k}} \quad \text{..... 7}$$

$$x_D = \frac{2x}{L}\sqrt{\frac{k}{k_x}} \quad \text{..... 8}$$

$$x_{eD} = \frac{2x_e}{L}\sqrt{\frac{k}{k_x}} \quad \text{..... 9}$$

$$x_{wD} = \frac{2x_w}{L}\sqrt{\frac{k}{k_x}} \quad \text{..... 10}$$

$$y_D = \frac{2y}{L}\sqrt{\frac{k}{k_y}} \quad \text{..... 11}$$

$$y_{eD} = \frac{2y_e}{L}\sqrt{\frac{k}{k_y}} \quad \text{..... 12}$$

$$y_{wD} = \frac{2y_w}{L}\sqrt{\frac{k}{k_y}} \quad \text{..... 13}$$

$$z_D = \frac{2z}{L}\sqrt{\frac{k}{k_z}} \quad \text{..... 14}$$

$$z_{eD} = \frac{2z_e}{L}\sqrt{\frac{k}{k_z}} \quad \text{..... 15}$$

$$z_{wD} = \frac{2z_w}{L}\sqrt{\frac{k}{k_z}} \quad \text{..... 16}$$

$$d_x = D_x = \frac{x_e - L}{2} \quad \text{..... 17}$$

$$r_{wD} = \frac{z_{eD}}{2} - z_{wD} \quad \text{..... 18}$$

$$P_D = \frac{kh\Delta P}{141.2q\mu B_0} \quad \text{..... 19}$$

$$t_D = \frac{0.001056kt}{\phi\mu C_t L^2} \quad \text{..... 20}$$

$$x_w = \frac{x_e - L}{2} \quad \text{..... 21}$$

References

[1]. Chu H., Liao X., Chen Z., ZhaoX., Liu W., Dong P., 2019, " Transient pressure analysis of a horizontal well with multiple, arbitrarily shaped horizontal fractures", *Journal of Petroleum Science and Engineering Journal*. https://doi.org/10.1016/j.petrol.2019.06.003

[2]. Lu J., Rahman M.M., Yang E., Alhamami M. T., Zhong H., 2022, " Pressure transient behavior in a multilayer reservoir with formation crossflow", *Journal of Petroleum Science and Engineering.* Volume 208, Part B, January. https://doi.org/10.1016/j.petrol.2021.109376.

[3]. Viana I., Bela R.V., Pesco S., Barreto A. Jr, 2022, "An analytical model for pressure behavior in multilayered radially composite reservoir with formation crossflow", *Journal of Petroleum Exploration and Production Technology*. https://doi.org/10.1007/s13202-022-01460-x

[4]. Oloro J. and Adewole E.S., 2015, "Factors that affect pressure distribution of horizontal wells in a layered reservoir with simultaneous gas cap and bottom water drive", *Journal of Petroleum and Gas Engineering*. Vol. 6(1), pp. 1-9, January. DOI: 10.5897/JPGE 2013.0180

[5]. Falode O. A., Alawode A. J. and Sadam Y. D., 2018, 'State-of-Art Solution for Pressure Transient Analysis in Deviated Wells Penetrating Stratified Reservoirs With Crossflow", *Journal of Advances in Mathematics and Computer Science*, Volume 29(3): 1-24, 2018; Article no. JAMCS.37750. DOI: 10.9734/JAMCS/2018/37750.

[6]. Oloro J., Adewole.E.S. and Olafuyi.O.A., 2014, "Pressure Distribution of Horizontal Wells in a Layered Reservoir with Simultaneous Gas Cap and Bottom Water Drives", *American Journal of Engineering Research (AJER)*.Volume-03, Issue-12, 41-53.

[7]. Abdulkadhim S. T. and Al-Obaidi D. A., 2023, "A Review on Pressure Transient Analysis in Multilayer Reservoir: South Iraq Case Study", *Iraqi Geological Journal*. DOI: 10.46717/igj.56.2E.16ms-2023-11-21.

[8]. Wang J., Wang X., Dong W., 2017, "Rate decline curves analysis of multiple-fractured horizontal wells in heterogeneous reservoirs", *Journal of Hydrology*. Volume 553, October 2017, Pages 527-539. https://doi.org/10.1016/j.jhydrol.2017.08.024

[9] Goode, P. A. and Thambynayagam, R. K., 1987, "Pressure drawdown and buildup analysis of horizontal wells in anisotropic media". *SPE Formation Evaluation,* 683-697.

[10]. Li C., 2021, "Production Analysis for Fractured Vertical Well in Coal Seam Reservoirs with Stimulated Reservoir Volume", *Hindawi Geofluids*, Volume 2021, Article ID 1864734, 12 https://doi.org/10.1155/2021/1864734

[11]. Rbeawi S. A., Kadhim F. S., 2021, "The Impact of Completion Technology on Flow Dynamics and Pressure Behaviors of Horizontal Wells", *Iraqi Journal of Oil & Gas Research*, Vol. 1, No. 1

[12]. Jia, Z., Shi, B., Zhou, H., Chen, F., Meng, X., 2017, "Well path optimization technique for horizontal wells in reservoirs with ultra-low permeability and horizontal fractures", *Special Oil Reservoir* 24 (03), 151–154.

[13]. Luo, W., Tang, C., Wang, X., 2014a, "Pressure transient analysis of a horizontal well intercepted by multiple non-planar vertical fractures", *Journal of Petro. Sci. Eng*. 124, 232–242.

[14]. Luo, W., Wang, L., 2014b, "A novel semi-analytical model for horizontal fractures with non-Darcy flow", *Journal of Petroleum Sci. Eng*. 122, 166–172.

[15]. Oloro J., and Adewole.E.S. 2020, "Performance and Behavior of a Horizontal Well in Reservoir Subject to Double-Edged Water Drive", *Nigerian Journal of Technology (NIJOTECH).* Vol. 39, No. 2, April 2020, pp. 417 – 423. http://dx.doi.org/10.4314/njt.v39i2.11

[16]. Manriquez A. L., Sepehrnoori K., Cortes A. 2016, "A novel approach to quantify reservoir pressure along the horizontal section and to optimize multistage treatments and spacing between hydraulic fractures", *Journal of Petroleum Science and Engineering*. http://dx.doi.org/10.1016/j.petrol.2016.10.068

[17]. Ogbamikhumi A. V. and Adewole E.S., 2020, "Pressure Behaviour of a Horizontal Well Sandwiched Between Two Parallel Sealing Faults", *Nigerian Journal of Technology (NIJOTECH). Vol. 39, No. 1, January 2020, pp.* 148 – 153. http://dx.doi.org/10.4314/njt.v39i1.16

[18]. Kumar M., Sharma P., Gupta D. K. and Joshi V., 2015 "Application of Inflow Control Devices in Horizontal Well in Bottom Water Drive Reservoir using Reservoir Simulation", *International Journal of Engineering Research & Technology (IJERT*). Vol. 4 Issue 04,

[19]. Biryukov D. and Kuchuk F. J., 2015, 'Pressure Transient Behavior of Horizontal Wells Intersecting Multiple Hydraulic Fractures in Naturally Fractured Reservoirs", *Transp Porous Med* (2015) 110:369–408. DOI 10.1007/s11242-015-0554-1

[20]. Nguyen T.C., Pande S., Bui D., Al-Safran E. and Nguyen H.V., 2020, "Pressure dependent permeability: Unconventional approach on well performance', *Journal of Petroleum Science and* Engineering 193. https://doi.org/10.1016/j.petrol.2020.107358

[21] Odeh A. S. and Babu D.K., 1990, "Transient Flow Behavior of Horizontal Wells: Pressure Drawdown and Buildup Analysis", SPE Formation Evaluation, March, Pg 10-14.

[22] Gringarten A.C., and Ramey H.J.J r, ,1973, "The use of Source and Green's Functions in solving Unsteady-flow Problems in Reservoirs", *Society of Petroleum Engineers Journal, vol. 13, Pg.285-296.*

[23] Ozkan, E., Raghavan, R., and Joshi, S. D., 1989, "Horizontal well pressure analysis". SPEFE, 567.

[24] Chen Li, 2021, "Production Analysis for Fractured Vertical Well in Coal Seam Reservoirs with Stimulated Reservoir Volume", *Hindawi Geofluids*, Volume 2021, Article ID 1864734, 12 pages https://doi.org/10.1155/2021/186473

[25] Mutisya M. P., Adewole E. S., Otieno K. A. and Okang O. D., 2020, "A Mathematical Model for Pressure Distribution in a Bounded Oil ReservoirSubject to Single-Edged and Bottom Constant Pressure", *IOSR Journal of Mathematics (IOSR-JM). Volume 16, Issue 4 Ser. I (Jul.–Aug. 2020), PP 24-30*. DOI: 10.9790/5728-1604012430

[26] Ozkan, E., Raghavan, R., 1990, "Performance of Horizontal Wells Subject to Bottom water Drive", *SPE Res Eng* 5 (03): 375–383. Paper Number: SPE-18559-PA. https://doi.org/10.2118/18559-PA